

# TOWARDS MECHANISTIC INTERPRETABILITY OF GRAPH TRANSFORMERS VIA ATTENTION GRAPHS

**Batu El\***  
Stanford University  
batuel@stanford.edu

**Deepro Choudhury\***  
University of Oxford  
deepro.choudhury@stats.ox.ac.uk

**Pietro Liò**  
University of Cambridge  
pietro.liò@cl.cam.ac.uk

**Chaitanya K. Joshi**  
University of Cambridge  
chaitanya.joshi@cl.cam.ac.uk

## ABSTRACT

We introduce *Attention Graphs*, a new tool for mechanistic interpretability of Graph Neural Networks (GNNs) and Graph Transformers based on the mathematical equivalence between message passing in GNNs and the self-attention mechanism in Transformers. Attention Graphs aggregate attention matrices across Transformer layers and heads to describe how information flows among input nodes. Through experiments on homophilous and heterophilous node classification tasks, we analyze Attention Graphs from a network science perspective and find that: (1) When Graph Transformers are allowed to learn the optimal graph structure using all-to-all attention among input nodes, the Attention Graphs learned by the model do not tend to correlate with the input/original graph structure; and (2) For heterophilous graphs, different Graph Transformer variants can achieve similar performance while utilising distinct information flow patterns. Open source code: [github.com/batu-el/understanding-inductive-biases-of-gnns](https://github.com/batu-el/understanding-inductive-biases-of-gnns)

## 1 INTRODUCTION

Graph Neural Networks (GNNs) and Graph Transformers (GTs) have emerged as core deep learning architectures behind several recent breakthroughs in physical and life sciences (Zhang et al., 2023), with AlphaFold (Jumper et al., 2021) being the most prominent example. Despite their remarkable success, these models remain largely ‘engineering artifacts’, as noted by Demis Hassabis (Hassabis, 2024), requiring dedicated tools to interpret their underlying mechanisms and advance our scientific understanding (Lawrence et al., 2024). While significant progress has been made in mechanistic interpretability of regular transformers in natural language processing (Elhage et al., 2021; Bricken et al., 2023), similar tools for GNNs and GTs for scientific applications are currently lacking.

In this paper, we leverage the mathematical equivalence between message passing in GNNs and the self-attention mechanism in Transformers (Joshi, 2020; Vaswani et al., 2017) to investigate information flow patterns in these architectures. The core insight is that Graph Transformers produce two types of attention matrices: (1) matrices from different heads that capture distinct relationships between nodes, analogous to heterogeneous graphs; and (2) attention matrices across layers that represent how information flows through a dynamically evolving network over time. We introduce *Attention Graphs*, a principled framework that aggregates these attention matrices into a unified representation of information flow among input nodes, as illustrated in Figure 1. Through Attention Graphs, we utilize techniques from network science (Rathkopf, 2018; Krickel et al., 2023) to analyze how learned information flow patterns in GTs relate to the underlying graph structure. Based on the findings, we explore how different GT variants, which enforce graph structure to varying degrees, learn *distinct* information flow patterns despite performing similarly.

Our experiments across multiple architectures and node classification tasks reveal two key findings. First, when architectures do not explicitly constrain attention to the underlying graph structure

\*Equal contribution. Work done in [Geometric Deep Learning](#) course at the University of Cambridge.

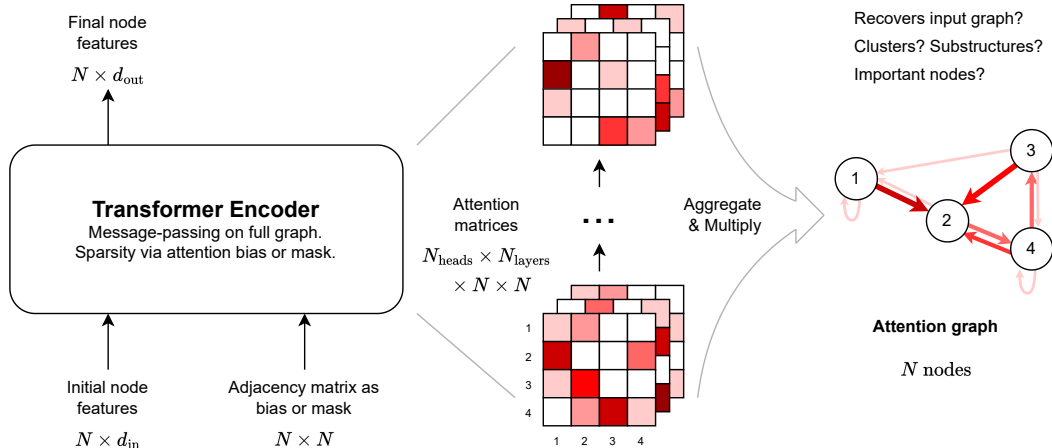


Figure 1: **Attention Graphs for mechanistic interpretability of GNNs and Graph Transformers.** *Left:* Graph Neural Networks are equivalent to Transformers operating on fully connected graphs (Joshi, 2020). *Middle:* The attention matrices at each layer and each head in the Transformer tell us how information flows among input tokens. *Right:* The attention matrices can be aggregated across layers and heads to construct a directed *Attention Graph* of information flow in the GNN/Graph Transformer. We can study Attention Graphs from a network science perspective to mechanistically understand the algorithms learned by GNNs and Graph Transformers.

provided as input, the learned information flow patterns deviate significantly from the input graph topology - this holds for both homophilous and heterophilous graphs (Platonov et al., 2023b). Secondly, on heterophilous graphs, different architectures can achieve similar performance while implementing *distinct* algorithmic strategies, as evidenced by their unique patterns of information flow. Moreover, we observe that certain nodes emerge as pivotal, disproportionately influencing predictions across the graph regardless of topological distance.

Overall, we have introduced the first framework for mechanistic interpretability of GNNs and GTs based on network science. While preliminary, this approach lays the foundation for future research toward understanding the algorithmic principles behind Transformers and attention-based models with the aim of unlocking deeper insights in their applications across the sciences. Our code is available via: [github.com/batu-el/understanding-inductive-biases-of-gnns](https://github.com/batu-el/understanding-inductive-biases-of-gnns).

## 2 PRELIMINARIES

**Graph Neural Networks.** A graph,  $G = (V, E)$ , is a mathematical structure that consists of a set of vertices  $V$  representing entities and a set of edges  $E \subseteq V \times V$  representing pairwise relationships between entities (Bronstein et al., 2021). A Graph Neural Network (GNN) for node classification learns a function  $f$  that maps nodes  $V$  to an associated set of class labels  $Y$  per node. Each node  $i$  is represented by an input feature vector  $x_i \in \mathbb{R}^d$ , where  $d$  is the feature dimension. We focus on graphs with binary relationships between nodes, characterized by an adjacency matrix  $A \in \mathbb{R}^{n \times n}$ , where  $a_{ij} = 1$  if nodes  $i$  and  $j$  are connected, and 0 otherwise. Thus, each graph is described by two matrices: the adjacency matrix  $A$  and the node feature matrix  $X \in \mathbb{R}^{n \times d}$ , where  $n$  is the number of nodes. The 1-hop neighbourhood of node  $i$  is defined as  $\mathcal{N}_i^1 = \{j \mid a_{ij} = 1\}$ . More generally, the  $k$ -hop neighborhood is  $\mathcal{N}_i^k = \{j \mid (A^k)_{ij} \neq 0\}$ , where  $A^k$  denotes the  $k$ -th power of  $A$ .

GNNs are the standard toolkit for deep learning on graph-structured data, using graph topology to propagate and aggregate information between connected nodes (Veličković, 2023). Unlike feed-forward networks (standard multi-layer perceptrons) which process each node independently via  $\text{MLP}(x_i) = y_i$ , GNNs use both the node features  $X$  and the graph structure  $A$  simultaneously when predicting node classes. Formally, a GNN implements a permutation-equivariant function  $f(X, A) = y$  such that  $f(\mathbf{P}X, \mathbf{P}A\mathbf{P}^T) = \mathbf{P}y$  for any permutation matrix  $\mathbf{P}$ . This permutation equivariance ensures the predictions for each node are invariant to node ordering.

**Message Passing.** GNN layers are implemented via message-passing (Battaglia et al., 2018) where nodes iteratively update their representations by aggregating information from their neighbors. Formally, a node’s representation  $h_i^\ell \in \mathbb{R}^{d_{\text{model}}}$  at layer  $\ell$  is updated to  $h_i^{\ell+1}$  via:

$$h_i^{\ell+1} = \phi\left(h_i^\ell, \bigoplus_{j \in \mathcal{N}_i^\ell} \psi(h_i^\ell, h_j^\ell, e_{ij})\right). \quad (1)$$

Here,  $\psi$  is a message function that determines how information flows between nodes  $i$  and  $j$  based on their representations and edge features  $e_{ij}$ ,  $\bigoplus$  is a permutation-invariant aggregation function (like sum or mean), and  $\phi$  is a node-wise update function that combines the aggregated messages with each node’s current representation.  $\psi$  and  $\phi$  are typically implemented as multi-layer perceptrons (MLPs) with learnable weights shared across all nodes. For the binary graphs in our experiments, edge features  $e_{ij}$  simply equal the corresponding entries  $a_{ij}$  in the adjacency matrix, though in general they can encode richer edge attributes.

Equation 1 provides a general formulation that encompasses most widely-used GNN architectures, including Graph Convolutional Networks (GCNs) (Kipf & Welling, 2017), Graph Isomorphism Networks (GINs) (Xu et al., 2019), and Message Passing Neural Networks (MPNNs) (Gilmer et al., 2017). We are particularly interested in attentional GNNs, where the message function  $\psi$  is implemented via the self-attention operation (Veličković et al., 2018; Brody et al., 2022). In this case, the message function  $\psi$  is a weighted sum of the representations of neighboring nodes, where the weights are computed using an attention mechanism.

$$\psi(h_i^\ell, h_j^\ell, e_{ij}) = \text{LocalAttention}(W^Q h_i^\ell, W^K h_j^\ell, W^V h_j^\ell) = \frac{\exp(Q_i^T K_j)}{\sum_{k \in \mathcal{N}_i^\ell} \exp(Q_i^T K_k)} \cdot V_j, \quad (2)$$

where  $Q_i = W^Q h_i^\ell$ ,  $K_j = W^K h_j^\ell$ ,  $V_j = W^V h_j^\ell$  are the query, key, and value vectors, respectively, and  $W^Q$ ,  $W^K$ ,  $W^V$  are learnable weight matrices. In practice, we use multi-head attention to project the node representations into multiple subspaces and compute attention in parallel, followed by concatenation and a final linear transformation.

**Graph Transformers.** GNNs and Transformers have deep mathematical connections (Joshi, 2020). Transformers are attentional GNNs operating on fully-connected graphs, where self-attention models relationships between all pairs of input tokens (Vaswani et al., 2017), i.e. graph nodes:

$$h_i^{\ell+1} = \phi\left(h_i^\ell, \bigoplus_{j \in \mathcal{V}} \psi(h_i^\ell, h_j^\ell, e_{ij})\right) = \text{FFN}\left(h_i^\ell + \sum_{j \in \mathcal{V}} \psi(h_i^\ell, h_j^\ell, e_{ij})\right), \quad (3)$$

$$\psi(h_i^\ell, h_j^\ell, e_{ij}) = \text{GlobalAttention}(W^Q h_i^\ell, W^K h_j^\ell, W^V h_j^\ell) = \frac{\exp(Q_i^T K_j)}{\sum_{k \in \mathcal{V}} \exp(Q_i^T K_k)} \cdot V_j. \quad (4)$$

This ability to attend to and gather information from all nodes allows Transformers to learn complex long-range dependencies without being constrained by a pre-defined graph structure or suffering from oversquashing bottlenecks (Di Giovanni et al., 2023).

Conversely, GNNs are Transformers where self-attention is restricted to local neighborhoods (Buterez et al., 2024), as formalized in equation 2, which can be realized in equation 3 by setting the message/attention weights to zero for any nodes  $i$  and  $j$  that are not connected in the graph, i.e. masking the attention. These insights have given rise to Graph Transformers (GTs) that generalize Transformers for graph-structured data (Dwivedi & Bresson, 2021; Müller et al., 2023). GTs aim to overcome oversquashing in GNNs by allowing global attention while still leveraging graph structure as an inductive bias (Rampásek et al., 2022).

**Attention Matrices in Graph Transformers.** Each GT layer performs a message passing operation as in equation 3, where the message function  $\psi$  is implemented via the global self-attention operation in equation 4. We can thus define an attention matrix  $\mathbb{A} \in \mathbb{R}^{n \times n}$  at each layer as a function of  $H$  and  $A$ , where  $H^\ell \in \mathbb{R}^{n \times d_{\text{model}}}$  contains the representation of a node from the graph in each of its rows and  $A$  is the adjacency matrix. A GT with  $N_L$  layers and  $N_H$  attention heads per layers will result in  $N_L \times N_H$  attention matrices every time the model is run on an input.

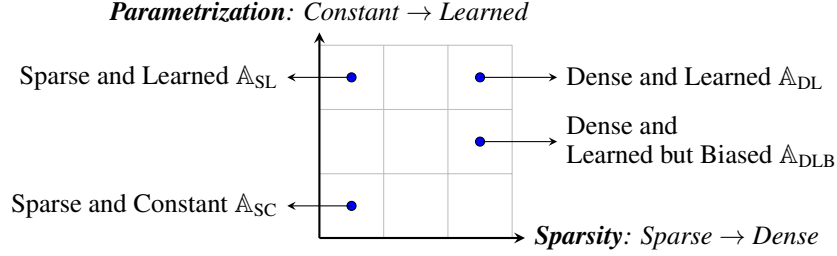


Figure 2: **Design space of Graph Transformers** based on two key dimensions: (1) sparsity of attention (sparse vs. dense) and (2) parametrization of attention (constant vs. learned).

### 3 ATTENTION GRAPHS FRAMEWORK

Processing graph-structured data through GNNs and GTs results in multiple attention matrices - one for each attention head in each layer. To understand these models, we need a principled approach to aggregate these matrices into a single *Attention Graph* that captures the overall information flow among nodes. In this section, we first formalize a unified design space of GNNs and GTs based on their attention mechanisms, and then introduce our framework for constructing and analyzing Attention Graphs to reveal the algorithmic patterns learned by different architectures.

#### 3.1 DESIGN SPACE OF GRAPH TRANSFORMERS

Having established the connection between GTs and GNNs through the attention mechanism and resulting attention matrices, we can formalise a spectrum of architectures based on two key dimensions: the *parametrization* and *sparsity* of the attention matrix  $\mathbb{A}$ . The parametrization dimension refers to whether the attention matrix is fixed or learned, while the sparsity dimension refers to whether the attention matrix is restricted to the neighborhood of the node or is allowed to be dense/global. Figure 2 visualizes these dimensions.

**Sparse and Constant (SC):** The attention matrix is sparse and fixed, with attention coefficients inversely proportional to the square root of the degree of the node being attended to, recovering GCNs (Kipf & Welling, 2017). The layer-wise update equation is:

$$h_i^{\ell+1} = \text{FFN}\left(h_i^\ell + \sum_{j \in \mathcal{N}_i^1} \frac{1}{\sqrt{d_i d_j}} \cdot V_j\right). \quad (5)$$

**Sparse and Learned (SL):** The attention matrix is sparse but learned, with attention coefficients learned as a function of the node features, recovering GATs (Veličković et al., 2018; Brody et al., 2022). The layer-wise update equation is:

$$h_i^{\ell+1} = \text{FFN}\left(h_i^\ell + \sum_{j \in \mathcal{N}_i^1} \frac{\exp(Q_i^T K_j)}{\sum_{k \in \mathcal{N}_i^1} \exp(Q_i^T K_k)} \cdot V_j\right). \quad (6)$$

**Dense and Learned but Biased (DLB):** The attention matrix is dense and learned, but biased to be inversely proportional to the shortest path length between the nodes, recovering the Graphormer (Ying et al., 2021). The layer-wise update equation is:

$$h_i^{\ell+1} = \text{FFN}\left(h_i^\ell + \sum_{j \in V} \frac{\exp(Q_i^T K_j + b_{ij})}{\sum_{k \in V} \exp(Q_i^T K_k + b_{ij})} \cdot V_j\right), \quad (7)$$

where the bias term  $b_{ij} = 1/\text{shortest path length between nodes } i \text{ and } j$  encourages the model to attend to nodes that are closer in the graph without enforcing a strict neighborhood structure.

**Dense and Learned (DL):** The attention matrix is dense and learned in an unbiased manner, akin to the Transformer attention mechanism (Vaswani et al., 2017). This is the most flexible model that

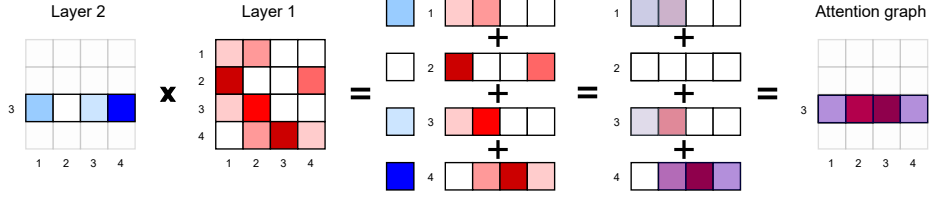


Figure 3: **Aggregating attention across layers by matrix multiplication.** Attention matrices from successive layers are combined to capture indirect information flow. For node  $i$ , row  $i$  in the attention matrix  $\mathbb{A}_{L_2}$  represents how much it attends to each intermediate node  $j$ . Each row  $j$  in  $\mathbb{A}_{L_1}$  captures how those intermediate nodes attend to other nodes  $k$ . Matrix multiplication  $\mathbb{A}_{L_2}\mathbb{A}_{L_1}$  combines these patterns, revealing how node  $i$  indirectly attends to node  $k$  through intermediate nodes  $j$ .

allows each node to attend to every other node in the graph without any graph structure bias. The layer-wise update equation is:

$$h_i^{\ell+1} = \text{FFN}\left(h_i^\ell + \sum_{j \in V} \frac{\exp(Q_i^T K_j)}{\sum_{k \in V} \exp(Q_i^T K_k)} \cdot V_j\right), \quad (8)$$

All these models can be implemented using the same Transformer architecture, with the only difference being the attention mechanism used in the message passing operation. In practice, we use the PyTorch module `torch.nn.TransformerEncoder` to implement all models, with the main difference being the attention mask and/or bias used (Buterez et al., 2024; Dong et al., 2024).

### 3.2 AGGREGATING ATTENTION ACROSS HEADS AND LAYERS

To understand how information flows within GNNs and Graph Transformers, we need to combine multiple attention matrices: (1) attention matrices from different heads, which can be viewed as capturing different types of relationships between nodes, similar to heterogeneous graphs; and (2) attention matrices across layers, which represent how information flows through a dynamically evolving network over time. This section presents our framework for aggregating these matrices into a single Attention Graph that reveals the overall information flow patterns in the model.

**Aggregating attention across heads.** Attention matrices across heads can be viewed as representing different types of relationships between nodes, analogous to edge types in heterogeneous graphs. To enable systematic analysis, we need to combine these relationships into a single homogeneous graph whose edges capture the aggregate information flow from all attention heads at a given layer. We first examine whether different heads learn similar or distinct attention patterns in Appendix Figure 6, which shows pairwise correlations between attention values learned by different heads in 1-layer 2-head variants of our models defined in Section 3.1. For homophilous datasets, SL models exhibit strong positive correlations between heads, indicating they converge on similar attention patterns. This correlation remains positive but weaker for heterophilous datasets in both SL (row 1) and DLB models (row 2). DL models (row 3) show the weakest correlations, though still consistently positive. Crucially, we never observe negative correlations between heads, suggesting they learn complementary rather than competing patterns.

These intuitive observations motivate aggregating across heads through simple averaging:  $\mathbb{A}_{\text{Agg}} = \frac{1}{N_H} \sum_{i=1}^{N_H} \mathbb{A}_{H_i}$ , where  $N_H$  is the number of heads and  $\mathbb{A}_{H_i}$  is the attention matrix for head  $i$ . While straightforward, this averaging approach effectively captures the overall information flow patterns learned by multi-head attention without losing important signals from any individual head.

**Aggregating attention across layers.** Attention matrices across layers capture how information flows through the network over multiple message passing steps, forming dynamic graphs that evolve temporally. Our goal is to aggregate these matrices into a single Attention Graph that captures the overall flow of information across all layers of the model. We analyzed the correlation between attention patterns in different layers in Appendix Figure 7, which shows pairwise correlations between attention values learned in first and second layers of 2-layer 1-head models. We observed positive but weaker correlations compared to across-head patterns. This suggests that simple averaging

may not be sufficient for combining attention across layers, necessitating a more nuanced approach that captures how information propagates through the network.

We propose using matrix multiplication of attention matrices from successive layers to model the information flow from successive layers (illustrated in Figure 3):

$$\mathbb{A}_{\text{Agg.}} = \mathbb{A}_{L_2} \mathbb{A}_{L_1}, \quad (9)$$

This formulation elegantly captures indirect attention patterns: if node  $i$  attends to node  $j$  in layer 2, it indirectly attends to all nodes that  $j$  attended to in layer 1. Mathematically, row  $i$  of  $\mathbb{A}_{\text{Agg.}}$  represents a linear combination of rows in  $\mathbb{A}_{L_1}$ , weighted by attention coefficients in row  $i$  of  $\mathbb{A}_{L_2}$ . This multiplication operation naturally models multi-hop information flow - for example, if node  $j$  attends to  $k$  in layer 1 and node  $i$  attends to  $j$  in layer 2, the matrix product captures the indirect flow of information from  $k$  to  $i$  through the intermediate node  $j$ .

**Constructing the Attention Graph.** After performing a forward pass through the model, we obtain attention matrices  $\mathbb{A}_{\ell h}$  for each layer  $\ell$  and head  $h$ . To construct the Attention Graph, we first aggregate attention across heads at each layer to obtain layer-wise attention matrices  $\mathbb{A}_{\ell}$ , then multiply these matrices sequentially across layers to construct the final aggregate attention matrix  $\mathbb{A}_{\text{Agg.}}$ . This process captures the overall information flow patterns learned by the model, revealing how information propagates through the network over time.

## 4 EXPERIMENTS

### 4.1 EXPERIMENTAL SETUP

**Datasets.** We evaluate our framework on 7 node classification datasets with varying levels of homophily, with further details in Appendix A. The datasets include: (1) *Citation Networks (Homophilous)*: Cora and Citeseer (Yang et al., 2016), where nodes represent scientific papers (with bag-of-words features from abstracts), edges represent citations, and classes are research topics. (2) *Wikipedia Networks (Heterophilous)*: Chameleon and Squirrel (Roemberczki et al., 2019), where nodes are Wikipedia articles (with noun presence features), edges are hyperlinks, and classes are based on monthly traffic. (3) *University Webpages (Heterophilous)*: Cornell, Texas, and Wisconsin from WebKB (Pei et al., 2020), where nodes are university webpages (with bag-of-words features), edges are hyperlinks, and classes are webpage categories.

**Models.** We experiment with four variants of Graph Transformers defined in Section 3.1: SC, SL, DLB, and DL. These models span a spectrum of attention mechanisms, from sparse and fixed to dense and learned, allowing us to systematically analyze the impact of different inductive biases on the information flow patterns learned by the model. We use the Transformer Encoder module in PyTorch to implement all models, with the only difference being the attention mask and/or bias used. We experiment with number of layers  $N_L \in \{1, 2\}$  and number of heads  $N_H \in \{1, 2\}$ , resulting in 4 model variants for each dataset (described subsequently). We set the hidden dimension  $d_{\text{model}} = 128$  for all models, resulting in node representations  $H^\ell \in \mathbb{R}^{n \times 128}$ .

**Node classification performance** Before analyzing the mechanistic interpretability of our models, we first evaluate their performance on node classification tasks. While achieving state-of-the-art performance is not our primary goal, we verify that our models are competitive with existing approaches. As shown in Appendix Table 3, we observe distinct performance patterns across different graph types: (1) On homophilous graphs (Cora, Citeseer), models that restrict attention to local neighborhoods (SC, SL) achieve the highest accuracy. (2) On heterophilous graphs (Cornell, Texas, Wisconsin), removing neighborhood constraints (DL) leads to better performance, suggesting the importance of long-range interactions. (3) On moderately homophilous graphs (Chameleon, Squirrel), biasing attention towards neighbors without strict restrictions (DLB) achieves optimal results. Notably, these performance patterns remain consistent across different model configurations, with minimal variation when increasing the number of attention heads or layers.

### 4.2 HOW DO GRAPH TRANSFORMERS DISTRIBUTE ATTENTION?

Figure 4 visualizes how different GT variants distribute attention between neighboring and non-neighboring nodes. In single-layer SL models, nodes can only attend to their immediate neighborhood

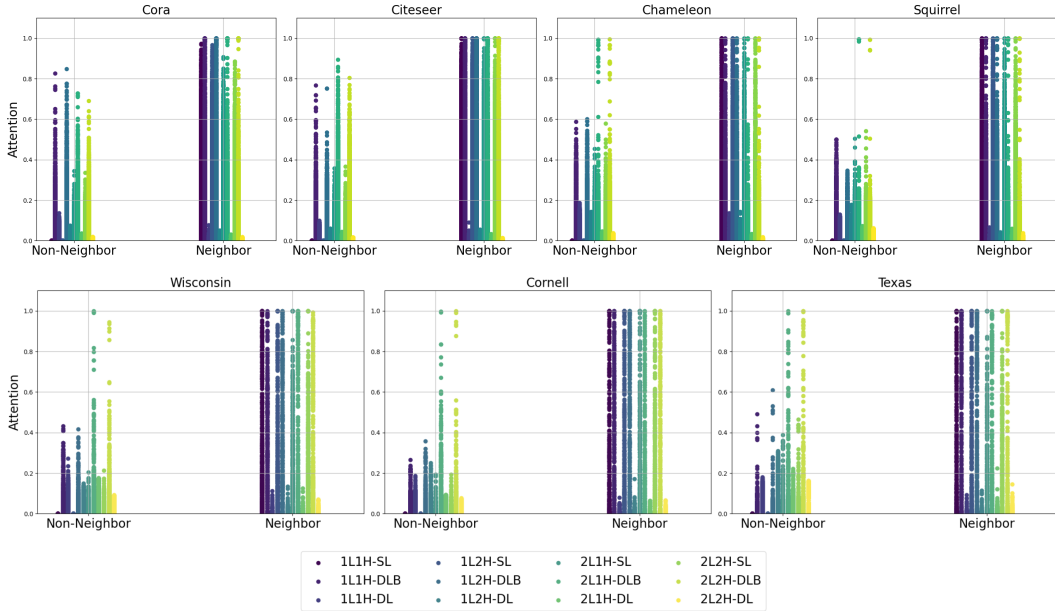


Figure 4: **Distribution of attention between neighbors and non-neighbors across different Graph Transformer architectures.** For SL (Sparse Learned), DLB (Dense Learned with Bias), and DL (Dense Learned) models, we visualize the attention patterns for four configurations: 1-layer 1-head, 1-layer 2-head, 2-layer 1-head, and 2-layer 2-head. Each point represents the weight of attention paid by a node in the aggregated Attention Graph, and whether it attends to a neighbor or non-neighbor from the input graph. DLB models mostly attend to neighbors, while DL models distribute attention more uniformly between neighbors and non-neighbors.

due to the architectural constraint. However, in two-layer models, attention to non-neighbors emerges naturally through information propagation across the network - a phenomenon effectively captured by our attention aggregation framework. DLB models, with their graph-biased attention, concentrate most of their attention within local neighborhoods. In contrast, DL models distribute attention roughly uniformly between neighbors and non-neighbors, as quantified in Appendix Table 4 through the ratio of average attention paid to non-neighbors versus neighbors. To examine these patterns more granularly, Appendix Figure 8 breaks down attention distribution by n-hop distances for 1-layer 1-head models. This analysis reveals that DLB models exhibit strong locality bias with attention decaying sharply with hop distance, while DL models maintain relatively uniform attention across all  $k$ -hop neighborhoods, suggesting fundamentally different information aggregation strategies.

### 4.3 DO GRAPH TRANSFORMERS RECOVER INPUT GRAPH STRUCTURE?

Next we check whether the learned attention in our dense models matches the underlying graph structure. We construct quasi-adjacency matrices by thresholding Attention Graphs to recover binary connectivity patterns, as described in Appendix B. Table 1 compares the quasi-adjacency matrices against original adjacency matrices using F1-scores. Low F1-scores (<4%) for DL models across all datasets indicate their attention patterns do not reflect the input graph structure. In contrast, DLB models show moderate to high F1-scores (28-86%), suggesting they partially recover graph connectivity through biased attention. Multi-head models generally achieve higher F1-scores, likely because averaging across heads reduces noise in learned attention patterns. However, for both architectures, F1-scores decrease with model depth, indicating that deeper layers develop more complex information flow patterns beyond the original graph structure.

### 4.4 A CLOSER LOOK AT QUASI-ADJACENCY MATRICES

Finally, we analyze the quasi-adjacency matrices to understand information flow patterns across different architectures. Figure 9 reveals three key findings:

Table 1: **Comparing graph structure recovery between DLB and DL models** using F1-scores between original adjacency matrices and thresholded attention matrices. Higher F1-scores indicate better preservation of the original graph structure in the model’s learned attention patterns. DL models consistently achieve lower F1-scores compared to DLB models, suggesting they do not recover the input graph structure.

	1L1H		1L2H		2L1H		2L2H	
	DLB	DL	DLB	DL	DLB	DL	DLB	DL
Cora	46.75	0.13	61.58	0.38	36.58	0.21	37.94	0.32
Citeseer	28.24	0.22	41.51	0.69	33.70	0.23	39.02	0.13
Chameleon	51.01	0.76	58.63	0.72	28.32	1.24	33.98	0.39
Squirrel	84.11	0.07	86.31	0.07	49.22	0.43	50.10	0.51
Cornell	57.44	0.21	61.38	0.85	43.51	1.25	48.95	1.04
Texas	58.37	0.61	58.31	1.22	44.83	3.69	47.14	2.95
Wisconsin	58.06	1.48	58.78	0.95	41.94	1.06	41.12	1.47

**1. Strong Self-Attention in Dense and Learned but Biased Models:** The quasi-adjacency matrices learned by DLB models show prominent diagonal patterns, particularly in two-layer configurations, indicating nodes primarily attend to themselves. This suggests these models may solve the classification task by focusing on initial node features rather than extensively aggregating information from neighboring nodes, especially for heterophilous graphs where local structure is less informative.

**2. Reference Nodes in Dense and Learned Models:** In contrast, DL models consistently exhibit distinct vertical patterns in their quasi-adjacency matrices across all datasets, suggesting the emergence of "reference nodes" that receive high attention from all other nodes. These patterns become more pronounced in two-layer models and larger heterophilous graphs like Chameleon and Squirrel. We hypothesize that DL models implement a classification algorithm based on comparing nodes against these learned reference nodes rather than relying on local graph structure. This finding is also supported by the benefits of including global/virtual nodes or register tokens in GTs (Gilmer et al., 2017; Darcet et al., 2024).

**3. Distinct Algorithms, Similar Performance:** Most notably, while DLB and DL models achieve comparable accuracy on heterophilous tasks (Table 3), their attention patterns reveal fundamentally different algorithmic strategies. This finding challenges the common practice of evaluating models solely based on accuracy metrics and highlights the importance of analyzing internal model behavior to understand learned computational strategies.

## 5 RELATED WORK

Our work bridges GNN explainability and mechanistic interpretability of Transformers, aiming to understand how information flows through these architectures during inference from the perspective of graph theory and network science (Rathkopf, 2018; Krickel et al., 2023).

**GNN Explainability.** Early work on explaining GNNs focused on identifying influential subgraphs for specific predictions (Ying et al., 2019). This spawned several approaches including concept-based methods (Magister et al., 2021), counterfactual explanations (Lucic et al., 2022), and generative explanations (Yuan et al., 2020). While valuable, these methods primarily analyze input-output relationships rather than internal model dynamics. Other work has investigated physical laws learned by GNNs using symbolic regression (Cranmer et al., 2020), but a systematic framework for understanding information flow in GNNs remains lacking.

**Mechanistic Interpretability of Transformers.** Recent advances in mechanistic interpretability aim to reverse-engineer neural networks into human-understandable components (Olah, 2022; Elhage et al., 2021). This has led to breakthroughs in understanding model features (Olah et al., 2017; Elhage et al., 2022), identifying computational circuits (Nanda et al., 2023; Cammarata et al., 2020), and explaining emergent behaviors (Barak et al., 2023; Wei et al., 2022). These insights have practical benefits - enabling better out-of-distribution generalization (Mu & Andreas, 2021), error correction (Hernandez et al., 2022), and prediction of model behavior (Meng et al., 2022). Our work aims



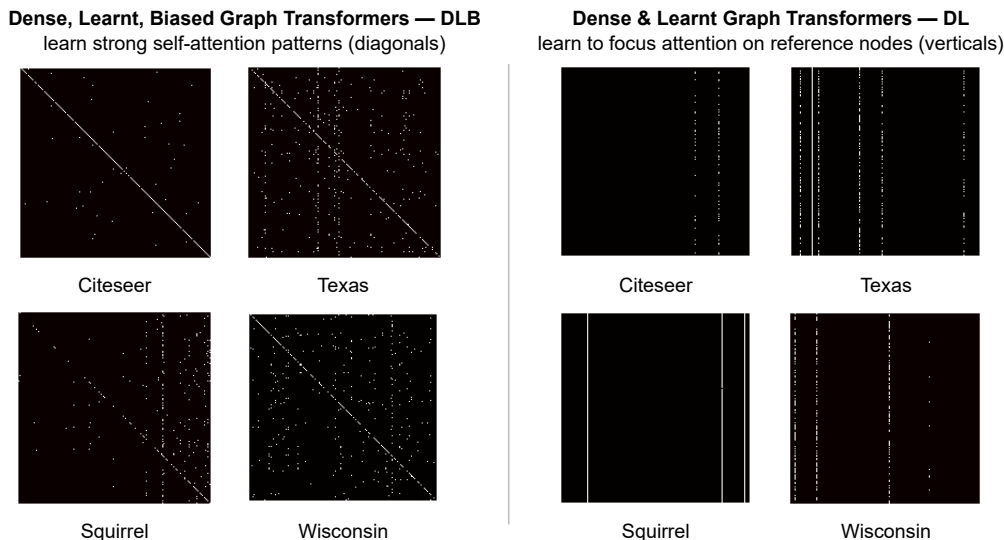


Figure 5: **Different graph inductive biases lead to distinct algorithmic strategies.** We plot quasi-adjacency matrices derived from Attention Graphs for DLB and DL models across different datasets for the 2-layer 2-head configuration. Black squares indicate no edges in the thresholded Attention Graph, while white squares indicate edges. DLB models exhibit strong self-attention patterns (diagonal lines), suggesting they focus on initial node features rather than aggregating information from neighbors. DL models develop reference nodes (vertical lines) that receive high attention from all other nodes, suggesting a classification algorithm based on comparing nodes against these references. See Figure 9 for all model configurations and datasets.

to extend the principles of mechanistic interpretability to GNNs by leveraging their mathematical connection to Transformers. A complementary effort is emerging around mechanistic interpretability of biological language models (Zhang et al., 2024; Simon & Zou, 2024; Adams et al., 2025), sharing our goal of extracting scientific insights from AI systems trained on structured scientific data.

## 6 DISCUSSION

In this paper, we developed a framework to mechanistically interpret GNNs and Graph Transformers by analyzing their attention patterns from the perspective of network science. While previous work on Transformer circuits focused on discrete feature interactions (Bricken et al., 2023; Meng et al., 2022), our approach captures continuous information flow patterns between nodes through Attention Graphs. Through this lens, we demonstrated that architectures with different graph inductive biases can achieve similar performance while implementing distinct algorithmic strategies. This observation challenges the common practice of evaluating models solely based on accuracy metrics and highlights the need for more holistic evaluation approaches.

Our framework has important limitations to address in future work. First, while matrix multiplication effectively models indirect attention flow, it may not capture non-linear interactions from activation functions between layers. Second, aggregating heterogeneous attention patterns across heads and temporal patterns across layers into a single matrix may oversimplify complex model dynamics. Additionally, our preliminary experiments are currently limited to small models (up to 2 layers, 2 heads) and node classification tasks where homophily analysis provides clear insights into the importance of graph structure. Future work should extend the Attention Graph framework to more complex graph architectures and inductive tasks to develop a more complete understanding of information flow in Graph Transformers. Attention Graphs opens up numerous directions for applying network science and graph theory to analyze Transformers, including spectral analysis, community detection, and information flow dynamics. These tools could reveal deeper insights into the emergent computational strategies learned by these models.

---

## ACKNOWLEDGEMENTS

We would like to thank Petar Veličković, Dobrik Georgiev, and Jonas Jürß for helpful discussions. BE is supported by the Knight-Hennessy Scholarship. DC is supported by the Oxford-Radcliffe PhD Scholarship and an EPSRC PhD Studentship for the StatML Centre for Doctoral Training. CKJ is supported by the A\*STAR Singapore National Science Scholarship (PhD) and the Qualcomm Innovation Fellowship.

## REFERENCES

- Sami Abu-El-Haija, Bryan Perozzi, Amol Kapoor, Hrayr Harutyunyan, Nazanin Alipourfard, Kristina Lerman, Greg Ver Steeg, and Aram Galstyan. Mixhop: Higher-order graph convolution architectures via sparsified neighborhood mixing. In *International Conference on Machine Learning (ICML)*, 2019.
- Etowah Adams, Liam Bai, Minji Lee, Yiyang Yu, and Mohammed AlQuraishi. From mechanistic interpretability to mechanistic biology: Training, evaluating, and interpreting sparse autoencoders on protein language models. *bioRxiv*, 2025.
- Boaz Barak, Benjamin L. Edelman, Surbhi Goel, Sham Kakade, Eran Malach, and Cyril Zhang. Hidden progress in deep learning: Sgd learns parities near the computational limit, 2023.
- Peter W. Battaglia, Jessica B. Hamrick, Victor Bapst, Alvaro Sanchez-Gonzalez, Vinicius Zambaldi, Mateusz Malinowski, Andrea Tacchetti, David Raposo, Adam Santoro, Ryan Faulkner, Caglar Gulcehre, Francis Song, Andrew Ballard, Justin Gilmer, George Dahl, Ashish Vaswani, Kelsey Allen, Charles Nash, Victoria Langston, Chris Dyer, Nicolas Heess, Daan Wierstra, Pushmeet Kohli, Matt Botvinick, Oriol Vinyals, Yujia Li, and Razvan Pascanu. Relational inductive biases, deep learning, and graph networks, 2018.
- Trenton Bricken, Adly Templeton, Joshua Batson, Brian Chen, Adam Jermyn, Tom Conerly, Nick Turner, Cem Anil, Carson Denison, Amanda Askell, Robert Lasenby, Yifan Wu, Shauna Kravec, Nicholas Schiefer, Tim Maxwell, Nicholas Joseph, Zac Hatfield-Dodds, Alex Tamkin, Karina Nguyen, Brayden McLean, Josiah E Burke, Tristan Hume, Shan Carter, Tom Henighan, and Christopher Olah. Towards monosemanticity: Decomposing language models with dictionary learning. *Transformer Circuits Thread*, 2023. <https://transformer-circuits.pub/2023/monosemantic-features/index.html>.
- Shaked Brody, Uri Alon, and Eran Yahav. How attentive are graph attention networks?, 2022.
- Michael M. Bronstein, Joan Bruna, Taco Cohen, and Petar Veličković. Geometric deep learning: Grids, groups, graphs, geodesics, and gauges, 2021.
- David Buterez, Jon Paul Janet, Dino Oglic, and Pietro Lio. Masked attention is all you need for graphs. *arXiv preprint arXiv:2402.10793*, 2024.
- Nick Cammarata, Shan Carter, Gabriel Goh, Chris Olah, Michael Petrov, Ludwig Schubert, Chelsea Voss, Ben Egan, and Swee Kiat Lim. Thread: Circuits. *Distill*, 2020. doi: 10.23915/distill.00024. <https://distill.pub/2020/circuits>.
- Miles Cranmer, Alvaro Sanchez Gonzalez, Peter Battaglia, Rui Xu, Kyle Cranmer, David Spergel, and Shirley Ho. Discovering symbolic models from deep learning with inductive biases. *Advances in neural information processing systems*, 2020.
- Timothée Darcet, Maxime Oquab, Julien Mairal, and Piotr Bojanowski. Vision transformers need registers. In *The Twelfth International Conference on Learning Representations*, 2024.
- Francesco Di Giovanni, Lorenzo Giusti, Federico Barbero, Giulia Luise, Pietro Lio, and Michael M Bronstein. On over-squashing in message passing neural networks: The impact of width, depth, and topology. In *International Conference on Machine Learning*, pp. 7865–7885. PMLR, 2023.
- Juechu Dong, Boyuan Feng, Driss Guessous, Yanbo Liang, and Horace He. Flex attention: A programming model for generating optimized attention kernels. *arXiv preprint arXiv:2412.05496*, 2024.
- Vijay Prakash Dwivedi and Xavier Bresson. A generalization of transformer networks to graphs, 2021.
- Nelson Elhage, Neel Nanda, Catherine Olsson, Tom Henighan, Nicholas Joseph, Ben Mann, Amanda Askell, Yuntao Bai, Anna Chen, Tom Conerly, Nova DasSarma, Dawn Drain, Deep Ganguli, Zac Hatfield-Dodds, Danny Hernandez, Andy Jones, Jackson Kernion, Liane Lovitt, Kamal Ndousse, Dario Amodei, Tom Brown, Jack Clark, Jared Kaplan, Sam McCandlish, and Chris Olah. A mathematical framework for transformer circuits. *Transformer Circuits Thread*, 2021. <https://transformer-circuits.pub/2021/framework/index.html>.

- 
- Nelson Elhage, Tristan Hume, Catherine Olsson, Nicholas Schiefer, Tom Henighan, Shauna Kravec, Zac Hatfield-Dodds, Robert Lasenby, Dawn Drain, Carol Chen, Roger Grosse, Sam McCandlish, Jared Kaplan, Dario Amodei, Martin Wattenberg, and Christopher Olah. Toy models of superposition, 2022.
- Justin Gilmer, Samuel S Schoenholz, Patrick F Riley, Oriol Vinyals, and George E Dahl. Neural message passing for quantum chemistry. In *ICML*, 2017.
- Demis Hassabis. Ai for science with sir paul nurse, demis hassabis, jennifer doudna, and john jumper. Google DeepMind: The Podcast, 2024. Quote: "You have to build the artifact of interest first, and then once you have it, you can then use the scientific method to reduce it down and understand its components."
- Evan Hernandez, Sarah Schwettmann, David Bau, Teona Bagashvili, Antonio Torralba, and Jacob Andreas. Natural language descriptions of deep visual features, 2022.
- Chaitanya Joshi. Transformers are graph neural networks. *The Gradient*, 2020. <https://thegradient.pub/transformers-are-graph-neural-networks/>.
- John Jumper, Ritchie Evans, Alexander Pritzel, and et al. Highly accurate protein structure prediction with alphafold. *Nature*, 596:583–589, 2021. doi: 10.1038/s41586-021-03819-2.
- Thomas N. Kipf and Max Welling. Semi-supervised classification with graph convolutional networks, 2017.
- Boris Knyazev, Graham W. Taylor, and Mohamed R. Amer. Understanding attention and generalization in graph neural networks, 2019.
- Beate Krickel, Leon de Bruin, and Linda Douw. How and when are topological explanations complete mechanistic explanations? the case of multilayer network models. *Synthese*, 2023.
- Elsa Lawrence, Adham El-Shazly, Srijit Seal, Chaitanya K Joshi, Pietro Liò, Shantanu Singh, Andreas Bender, Pietro Sormanni, and Matthew Greenig. Understanding biology in the age of artificial intelligence. *arXiv preprint*, 2024.
- Ana Lucic, Maartje ter Hoeve, Gabriele Tolomei, Maarten de Rijke, and Fabrizio Silvestri. Cf-gnnexplainer: Counterfactual explanations for graph neural networks, 2022.
- Lucie Charlotte Magister, Dmitry Kazhdan, Vikash Singh, and Pietro Liò. Gcexplainer: Human-in-the-loop concept-based explanations for graph neural networks, 2021.
- Kevin Meng, David Bau, Alex J Andonian, and Yonatan Belinkov. Locating and editing factual associations in GPT. In Alice H. Oh, Alekh Agarwal, Danielle Belgrave, and Kyunghyun Cho (eds.), *Advances in Neural Information Processing Systems*, 2022.
- Jesse Mu and Jacob Andreas. Compositional explanations of neurons, 2021.
- Luis Müller, Mikhail Galkin, Christopher Morris, and Ladislav Rampásek. Attending to graph transformers. *arXiv preprint*, 2023.
- Neel Nanda, Lawrence Chan, Tom Lieberum, Jess Smith, and Jacob Steinhardt. Progress measures for grokking via mechanistic interpretability. In *The Eleventh International Conference on Learning Representations*, 2023.
- M. E. J. Newman. Mixing patterns in networks. *Phys. Rev. E*, 2003.
- Chris Olah. Mechanistic interpretability, variables, and the importance of interpretable bases. <https://www.transformer-circuits.pub/2022/mech-interp-essay>, Jun 2022.
- Chris Olah, Alexander Mordvintsev, and Ludwig Schubert. Feature visualization. *Distill*, 2017. doi: 10.23915/distill.00007. <https://distill.pub/2017/feature-visualization>.
- Hongbin Pei, Bingzhe Wei, Kevin Chen-Chuan Chang, Yu Lei, and Bo Yang. Geom-gcn: Geometric graph convolutional networks. In *International Conference on Learning Representations*, 2020.
- Oleg Platonov, Denis Kuznedelev, Artem Babenko, and Liudmila Prokhorenkova. Characterizing graph datasets for node classification: Homophily-heterophily dichotomy and beyond. In *The Second Learning on Graphs Conference*, 2023a.
- Oleg Platonov, Denis Kuznedelev, Michael Diskin, Artem Babenko, and Liudmila Prokhorenkova. A critical look at the evaluation of GNNs under heterophily: Are we really making progress? In *The Eleventh International Conference on Learning Representations*, 2023b.

- 
- Ladislav Rampášek, Michael Galkin, Vijay Prakash Dwivedi, Anh Tuan Luu, Guy Wolf, and Dominique Beaini. Recipe for a general, powerful, scalable graph transformer. *Advances in Neural Information Processing Systems*, 2022.
- Charles Rathkopf. Network representation and complex systems. *Synthese*, 195:55–78, 2018.
- Benedek Rozemberczki, Carl Allen, and Rik Sarkar. Multi-scale attributed node embedding. *arXiv preprint*, 2019.
- Elana Simon and James Zou. Interplm: Discovering interpretable features in protein language models via sparse autoencoders. *bioRxiv*, 2024.
- Ashish Vaswani, Noam Shazeer, Niki Parmar, Jakob Uszkoreit, Llion Jones, Aidan N. Gomez, Lukasz Kaiser, and Illia Polosukhin. Attention is all you need, 2017.
- Petar Veličković. Everything is connected: Graph neural networks. *Current Opinion in Structural Biology*, 79: 102538, 2023.
- Petar Veličković, Guillem Cucurull, Arantxa Casanova, Adriana Romero, Pietro Liò, and Yoshua Bengio. Graph Attention Networks. In *ICLR*, 2018.
- Jason Wei, Yi Tay, Rishi Bommasani, Colin Raffel, Barret Zoph, Sebastian Borgeaud, Dani Yogatama, Maarten Bosma, Denny Zhou, Donald Metzler, Ed H. Chi, Tatsunori Hashimoto, Oriol Vinyals, Percy Liang, Jeff Dean, and William Fedus. Emergent abilities of large language models, 2022.
- Keyulu Xu, Weihua Hu, Jure Leskovec, and Stefanie Jegelka. How powerful are graph neural networks? In *ICLR*, 2019.
- Zhilin Yang, William W. Cohen, and Ruslan Salakhutdinov. Revisiting semi-supervised learning with graph embeddings. In *International Conference on International Conference on Machine Learning*, 2016.
- Chengxuan Ying, Tianle Cai, Shengjie Luo, Shuxin Zheng, Guolin Ke, Di He, Yanming Shen, and Tie-Yan Liu. Do transformers really perform badly for graph representation? In A. Beygelzimer, Y. Dauphin, P. Liang, and J. Wortman Vaughan (eds.), *Advances in Neural Information Processing Systems*, 2021.
- Rex Ying, Dylan Bourgeois, Jiaxuan You, Marinka Zitnik, and Jure Leskovec. Gnnexplainer: Generating explanations for graph neural networks, 2019.
- Hao Yuan, Jiliang Tang, Xia Hu, and Shuiwang Ji. Xggn: Towards model-level explanations of graph neural networks. In *International Conference on Knowledge Discovery and Data Mining*, 2020.
- Xuan Zhang, Limei Wang, Jacob Helwig, Youzhi Luo, Cong Fu, Yaochen Xie, Meng Liu, Yuchao Lin, Zhao Xu, Keqiang Yan, et al. Artificial intelligence for science in quantum, atomistic, and continuum systems. *arXiv preprint arXiv:2307.08423*, 2023.
- Zhidian Zhang, Hannah K. Wayment-Steele, Garyk Brixi, Haobo Wang, Matteo Dal Peraro, Dorothee Kern, and Sergey Ovchinnikov. Protein language models learn evolutionary statistics of interacting sequence motifs. *bioRxiv*, 2024. doi: 10.1101/2024.01.30.577970.
- Jiong Zhu, Yujun Yan, Lingxiao Zhao, Mark Heimann, Leman Akoglu, and Danai Koutra. Beyond homophily in graph neural networks: Current limitations and effective designs. In *Advances in Neural Information Processing Systems*, 2020.

## A DATASETS AND HOMOPHILY METRICS

We evaluate our framework on seven node classification datasets with varying levels of homophily. Table 2 summarizes the datasets and homophily metrics used in this paper. Homophily measures the likelihood of nodes with the same class label to connect with each other, providing insights into the underlying graph structure and the relationships between nodes.

Table 2: **Node classification datasets studied in this paper.** Homophily metrics range from -100 to 100, with higher values indicating stronger homophily (nodes of same class are more likely to connect). Number of classes indicates the number of unique labels per node.

Metric	Cora	Citeseer	Chameleon	Squirrel	Cornell	Texas	Wisconsin
Node Homophily	82.5	70.6	10.4	8.9	10.6	6.5	17.2
Edge Homophily	81.0	73.6	23.5	22.4	13.1	10.8	19.6
Adjusted Homophily	77.1	67.1	3.3	0.7	-21.1	-25.9	-15.2
Number of Nodes	2708	3327	2277	5201	183	183	251
Number of Edges	10556	9104	36101	217073	298	325	515
Number of Classes	7	6	5	5	5	5	5

**Node Homophily** computes, for each node, the fraction of its neighbors that share its class label, then averages across all nodes (Pei et al., 2020):

$$h_{\text{node}} = \frac{1}{|V|} \sum_{v \in V} \frac{|\{u \in N(v) : y_u = y_v\}|}{d(v)},$$

where  $V$  is the node set,  $N(v)$  contains the neighbors of node  $v$ ,  $y_v$  denotes  $v$ 's class label, and  $d(v)$  is  $v$ 's degree.

**Edge Homophily** calculates the fraction of edges that connect nodes of the same class (Zhu et al., 2020; Abu-El-Haija et al., 2019):

$$h_{\text{edge}} = \frac{|\{\{u, v\} \in E : y_u = y_v\}|}{|E|},$$

where  $E$  is the edge set. While intuitive, this metric can be misleading when class distributions are imbalanced.

**Adjusted Homophily** addresses class imbalance by comparing observed homophily against expected homophily given class proportions (Newman, 2003; Platonov et al., 2023a):

$$h_{\text{adj}} = h_{\text{edge}} - \frac{\sum_{k=1}^K \bar{p}(k)^2}{1 - \sum_{k=1}^K \bar{p}(k)^2},$$

where  $\bar{p}(k)$  represents the fraction of nodes in class  $k$ , and  $K$  is the total number of classes. This formula normalizes the difference between observed edge homophily  $h_{\text{edge}}$  and expected homophily  $\sum_{k=1}^K \bar{p}(k)^2$ , providing a more balanced measure of homophily in graphs with uneven class distributions.

## B QUASI-ADJACENCY MATRIX

To investigate whether learned attention patterns reflect the original graph structure, we convert aggregate Attention Graphs into binary "quasi-adjacency" matrices through thresholding. Following Knyazev et al. (2019), we set entries above a threshold to 1 and below to 0. The threshold is chosen such that the number of edges in the quasi-adjacency matrix approximately matches the original graph, helping balance precision and recall in our structure recovery analysis. We determine this threshold through grid search over  $[0,1]$  with 0.001 increments. This approach allows fair comparison between learned attention patterns and input graph structure while avoiding bias from overly sparse or dense quasi-adjacency matrices.

## C INTUITION FOR ATTENTION AGGREGATION ACROSS HEADS AND LAYERS

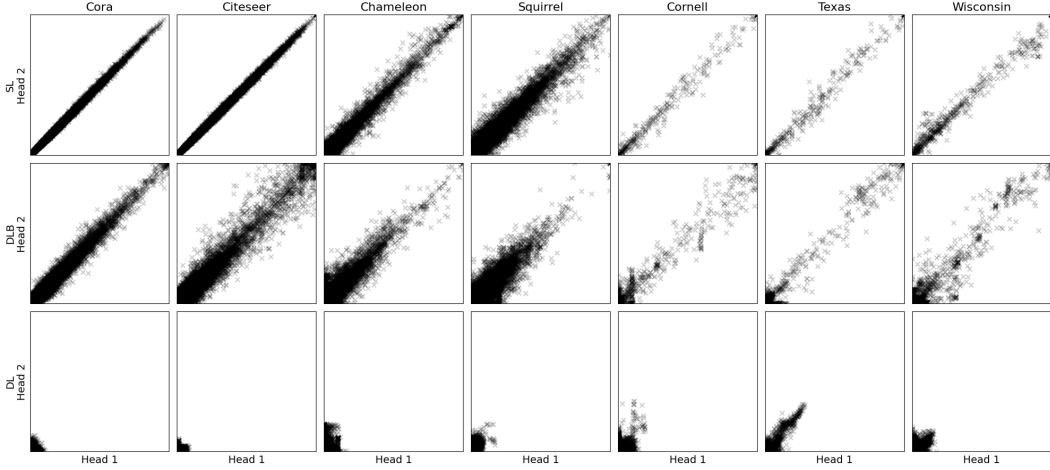


Figure 6: Comparison of attention patterns between heads in 1-layer 2-head transformer variants. Each point  $(x, y)$  represents the attention values  $(\mathbb{A}_{ij}^{H1}, \mathbb{A}_{ij}^{H2})$  from heads 1 and 2 respectively for the same node pair  $(i, j)$ . Points lying on  $x = y$  indicate identical attention patterns across heads, while deviations show head-specific specialization. We compare three architectures: SL (row 1, sparse learned attention), DLB (row 2, dense learned attention with graph bias), and DL (row 3, dense learned attention). Positive correlations suggest heads learn complementary rather than competing patterns.

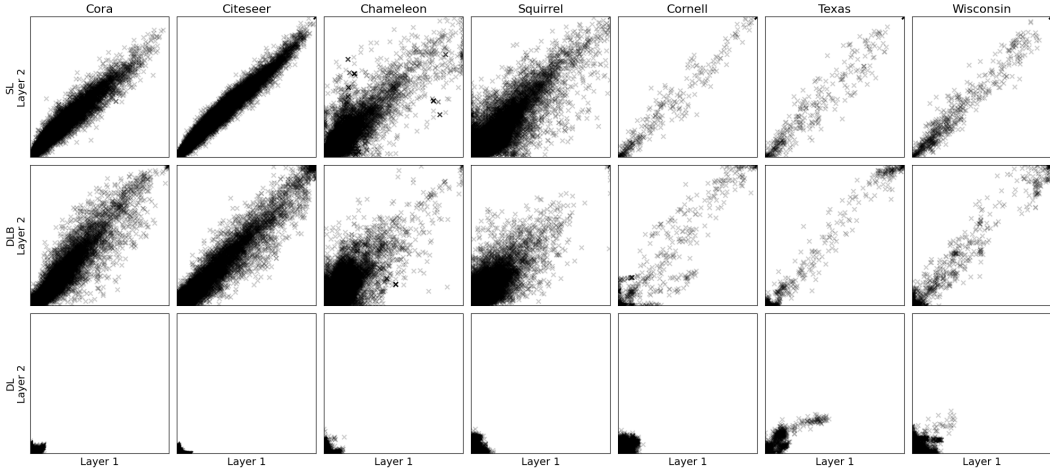


Figure 7: Comparison of attention patterns between layers in 2-layer 1-head transformer variants. Each point  $(x, y)$  represents the attention values  $(\mathbb{A}_{ij}^{L1}, \mathbb{A}_{ij}^{L2})$  from layers 1 and 2 respectively for the same node pair  $(i, j)$ . Points lying on  $x = y$  indicate identical attention patterns across layers, while deviations show layer-specific specialization. We compare three architectures: SL (row 1, sparse learned attention), DLB (row 2, dense learned attention with graph bias), and DL (row 3, dense learned attention). Layer-wise attention patterns show weaker correlations compared to head-wise patterns (Figure 6).

## D MODEL PERFORMANCE

Table 3: Model accuracies across different architectures and datasets. For each architecture (SC: Sparse Constant, SL: Sparse Learned, DLB: Dense Learned with Bias, DL: Dense Learned), we report mean accuracies across 10 runs with standard deviations in parentheses. Results highlighted in blue indicate best performing model(s) for each dataset. Training uses 40% of nodes for training, 30% for validation, and 30% for testing. SC models only use 1 head since they have constant attention patterns.

Model	Cora	Citeseer	Chameleon	Squirrel	Cornell	Texas	Wisconsin
1LIH							
SC	<b>0.85</b> (0.01)	<b>0.75</b> (0.02)	0.45 (0.02)	0.31 (0.01)	0.61 (0.05)	0.71 (0.06)	0.76 (0.05)
SL	<b>0.85</b> (0.01)	0.74 (0.02)	<b>0.57</b> (0.02)	<b>0.40</b> (0.01)	0.64 (0.03)	<b>0.78</b> (0.06)	0.79 (0.05)
DLB	<b>0.85</b> (0.01)	<b>0.75</b> (0.01)	<b>0.57</b> (0.02)	<b>0.40</b> (0.02)	0.65 (0.05)	0.77 (0.07)	0.80 (0.05)
DL	0.69 (0.02)	0.69 (0.02)	0.49 (0.02)	0.35 (0.01)	<b>0.69</b> (0.03)	0.75 (0.10)	<b>0.81</b> (0.04)
1L2H							
SL	<b>0.85</b> (0.01)	<b>0.74</b> (0.01)	<b>0.58</b> (0.02)	0.40 (0.01)	0.66 (0.07)	<b>0.78</b> (0.08)	0.78 (0.03)
DLB	0.84 (0.01)	<b>0.74</b> (0.02)	<b>0.58</b> (0.02)	<b>0.41</b> (0.01)	0.67 (0.05)	<b>0.78</b> (0.07)	0.78 (0.03)
DL	0.69 (0.02)	0.69 (0.01)	0.50 (0.02)	0.36 (0.01)	<b>0.71</b> (0.06)	<b>0.78</b> (0.04)	<b>0.80</b> (0.03)
2LIH							
SC	0.86 (0.01)	<b>0.75</b> (0.01)	0.43 (0.03)	0.32 (0.02)	0.60 (0.06)	0.66 (0.07)	0.71 (0.03)
SL	<b>0.87</b> (0.01)	0.74 (0.01)	0.60 (0.02)	<b>0.43</b> (0.01)	0.64 (0.05)	0.77 (0.07)	0.77 (0.03)
DLB	<b>0.87</b> (0.01)	<b>0.75</b> (0.01)	<b>0.61</b> (0.01)	<b>0.43</b> (0.02)	0.63 (0.09)	0.73 (0.08)	0.76 (0.05)
DL	0.69 (0.02)	0.69 (0.01)	0.50 (0.02)	0.36 (0.01)	<b>0.72</b> (0.06)	<b>0.79</b> (0.07)	<b>0.80</b> (0.03)
2L2H							
SL	<b>0.87</b> (0.01)	<b>0.74</b> (0.01)	0.61 (0.02)	<b>0.44</b> (0.01)	0.61 (0.07)	<b>0.77</b> (0.07)	0.75 (0.02)
DLB	0.86 (0.01)	<b>0.74</b> (0.01)	<b>0.63</b> (0.02)	<b>0.44</b> (0.01)	0.62 (0.09)	0.75 (0.07)	0.78 (0.04)
DL	0.69 (0.02)	0.69 (0.01)	0.50 (0.02)	0.36 (0.01)	<b>0.70</b> (0.06)	<b>0.77</b> (0.08)	<b>0.81</b> (0.03)

## E ATTENTION PATTERNS

Table 4: Comparing the relative attention distribution between local and global neighborhoods. For each model architecture and dataset, we compute the ratio of average attention paid to non-neighbors versus neighbors. A ratio of 0 indicates attention is strictly local (only within defined graph neighborhoods), while 1 indicates uniform attention distribution across all nodes regardless of connectivity. Ratios  $> 1$  suggest the model preferentially attends to nodes outside the local neighborhood. Self-attention is considered as within-neighborhood attention.

	Model	Cora	Citeseer	Chameleon	Squirrel	Cornell	Texas	Wisconsin
<b>1L1H</b>	SL	0.0	0.0	0.0	0.0	0.0	0.0	0.0
	DLB	0.0	0.0	0.01	0.0	0.01	0.0	0.0
	DT	1.13	0.68	1.03	1.16	1.28	1.21	0.86
<b>1L2H</b>	SL	0.00	0.00	0.00	0.00	0.00	0.00	0.00
	DLB	0.00	0.00	0.00	0.00	0.00	0.00	0.00
	DL	0.79	0.55	0.97	1.14	0.86	1.16	0.91
<b>2L1H</b>	SL	0.00	0.00	0.00	0.01	0.00	0.00	0.00
	DLB	0.00	0.00	0.02	0.02	0.01	0.01	0.01
	DL	0.96	0.77	0.94	1.25	1.00	0.75	0.98
<b>2L2H</b>	SL	0.00	0.00	0.00	0.01	0.00	0.00	0.00
	DLB	0.00	0.00	0.02	0.03	0.01	0.01	0.01
	DL	0.89	0.84	1.14	1.12	0.91	0.77	0.88

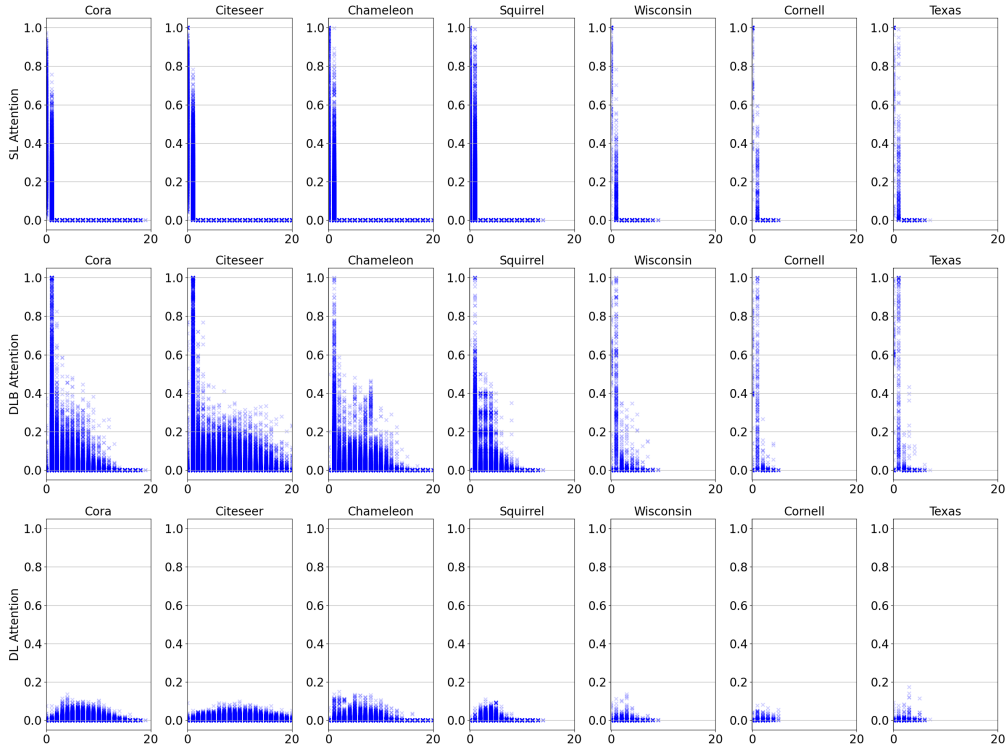


Figure 8: Distribution of attention values across n-hop neighborhoods in 1-layer 1-head models for SL (row 1), DLB (row 2), and DL (row 3). Each blue marker  $\times$  represents how much attention a node pays (y-axis) to nodes at different hop distances (x-axis). For example, if node  $i$  pays 0.5 attention to node  $j$  which is 3 hops away, this is plotted as point (3, 0.5). Self-attention (node attending to itself) is considered as 0-hop. Note how DLB models (row 2) focus attention on closer nodes while DL models (row 3) distribute attention more uniformly across all hop distances.



F EXTENDED FIGURE 5

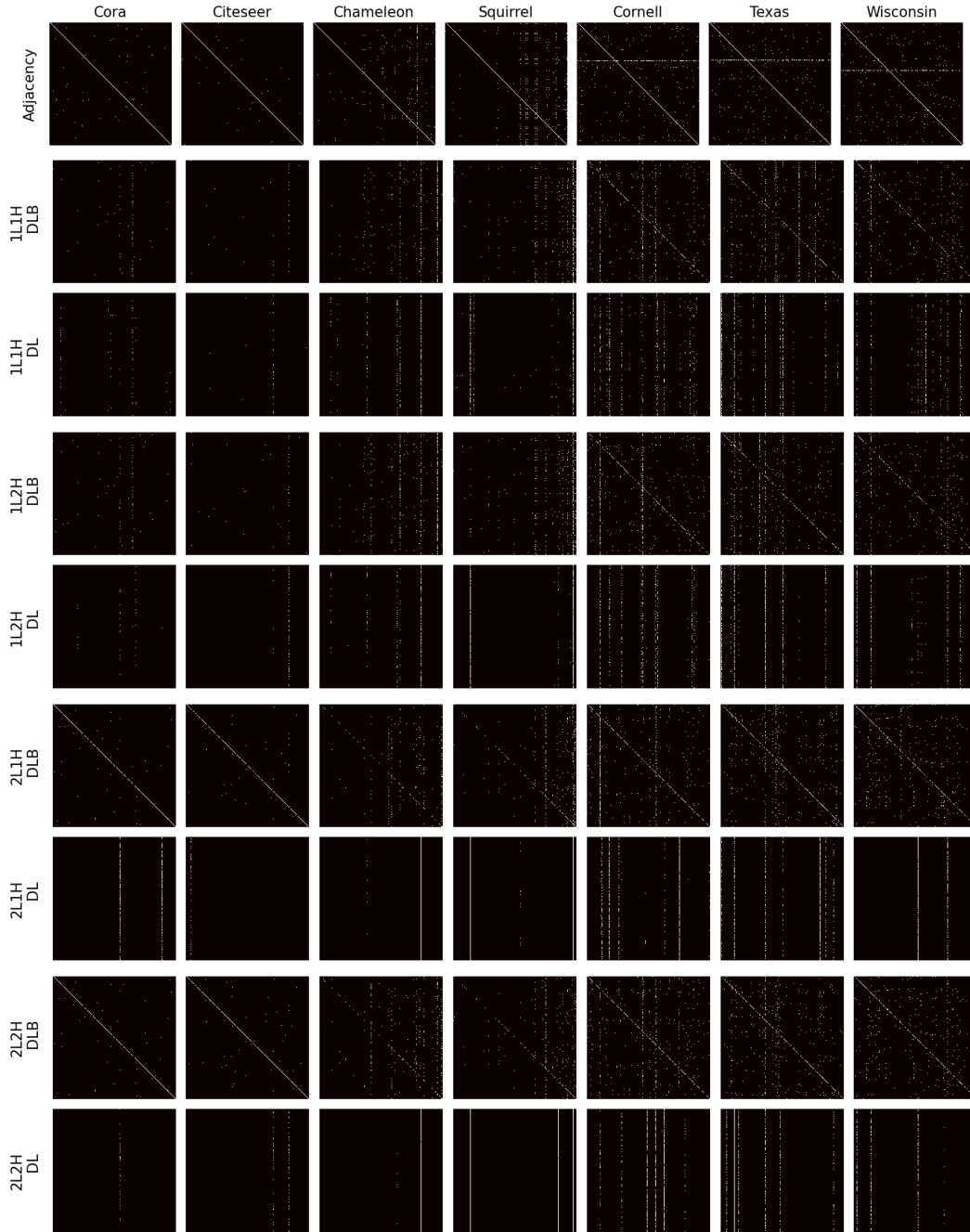


Figure 9: **Comparing adjacency and quasi-adjacency matrices across architectures and configurations.** Row 1: Original adjacency matrices for each dataset. Rows 2-9: Quasi-adjacency matrices constructed by thresholding Attention Graphs (see Appendix B) for different model configurations. These visualizations reveal distinct information flow patterns and algorithmic strategies learned by different architectures despite similar performance. DLB models exhibit strong self-attention patterns (diagonal lines), suggesting they focus on initial node features rather than aggregating information from neighbors. DL models develop reference nodes (vertical lines) that receive high attention from all other nodes, suggesting a classification algorithm based on comparing nodes against these references. Extended version of Figure 5.